Original Article

Dual-layer spectral computed tomography aortography using a seventy-five-percent-reduced iodine dose protocol and multiparameter spectral imaging: comparison with conventional computed tomography imaging

Aijie Wang[1#^], Wanjiang Li[1#^], Wenyu Huang[2^], Mao Luo[1^], Wendan Xiao[1^], Chaoyi Qin[3^], Shushan Dong[4^], Haiwei Liu[5^], Zhenlin Li[1*^], Kaiyue Diao[1*^]

[1]Department of Radiology, West China Hospital of Sichuan University, Chengdu, China; [2]West China School of Medicine, West China Hospital of Sichuan University, Chengdu, China; [3]Department of Cardiovascular Surgery, West China Hospital of Sichuan University, Chengdu, China; [4]Clinical Science, Philips Healthcare, Beijing, China; [5]Advanced Clinical Application, Philips Healthcare, Beijing, China

Contributions: (I) Conception and design: A Wang, W Li; (II) Administrative support: K Diao, C Qin, Z Li; (III) Provision of study materials or patients: M Luo, H Liu; (IV) Collection and assembly of data: A Wang, W Li; (V) Data analysis and interpretation: M Luo, W Xiao; (VI) Manuscript writing: All authors; (VII) Final approval of manuscript: All authors.

[#]These authors contributed equally to this work and should be considered as co-first authors.

[*]These authors contributed equally to this work as co-corresponding authors.

Correspondence to: Kaiyue Diao, MD. Department of Radiology, West China Hospital of Sichuan University, #37 Guoxue Alley, Wuhou District, Chengdu 610041, China. Email: kaiyuediao@wchscu.cn; Zhenlin Li, MD. Department of Radiology, West China Hospital of Sichuan University, #37 Guoxue Alley, Wuhou District, Chengdu 610041, China. Email: HX_lizhenlin@126.com.

Background: Computed tomography angiography (CTA) is the recommended diagnostic and follow-up imaging modality for acute aortic dissection (AD). However, the high-contrast medium burden associated with repeated CT aortography follow-ups remains a significant concern. This prospective study aimed to assess whether an ultra-low contrast dose (75% cutoff) aortic CTA protocol on dual-layer spectral CT could achieve comparable image quality with the full dose protocol. We also investigated the image quality of the virtual noncontrast (VNC) images derived from the ultra-low dose protocol.

Methods: This study included 37 consecutive patients who were referred to aortic CTA from May 2022 to August 2022. The enrolled patients underwent full-dose contrast CTA and ultra-low dose (reduced to 25% of conventional) contrast CTA on dual-layer spectral CT in 1 day. Virtual monochromatic images (VMIs) were reconstructed with 40 and 70 keV. The VNC images were reconstructed for both protocols. Objective image quality evaluation, recorded as signal-to-noise ratios (SNRs) and contrast-to-noise ratios (CNRs), was compared between the groups using 1-way analysis of variance and post hoc analysis with Bonferroni correction. Subjective image quality was also compared between the groups. Finally, VNC images derived from the low-dose (VNC_{low}) and full-dose (VNC_{full}) protocols were compared to the true noncontrast (TNC) images.

^ ORCID: Aijie Wang, 0000-0003-2368-3046; Wanjiang Li, 0000-0002-3488-6300; Wenyu Huang, 0000-0002-6794-022X; Mao Luo, 0000-0003-3514-5747; Chaoyi Qin, 0000-0001-7340-0628; Wendan Xiao, 0000-0002-2337-3147; Haiwei Liu, 0000-0002-7849-5264; Shushan Dong, 0000-0001-5466-7028; Zhenlin Li, 0000-0001-7525-330X; Kaiyue Diao, 0000-0002-6497-1020.

Results: Neither CNR nor SNR was lower for the 40-keV images reconstructed from the ultra-low dose group compared to the conventional images. Both were significantly higher than those of the 70-keV images. Regarding subjective image quality, vessel enhancement was not significantly different between the 40-keV VMI and full-dose images [ascending aorta (AAO): 4.37±0.46 *vs.* 4.57±0.48, P=0.096; brachiocephalic arteries: 4.34±0.45 *vs.* 4.51±0.49, P=0.152; abdominal aortic side branch: 4.42±0.48 *vs.* 4.51±0.49, P=0.480]. The VNC_{low} images were similar to the TNC images but significantly different from the VNC_{full} images (P<0.001).

Conclusions: Ultra-low contrast aortic CTA with a 75%-reduced iodine dose using dual-layer spectral CT and the derived VNC achieved image quality comparable to that of conventional CTA and TNC images.

Keywords: Aortic computed tomography aortography (aortic CTA); aortic dissection (AD); dual-layer spectral CT (DLCT); virtual noncontrast images (VNC images)

Submitted Jan 26, 2023. Accepted for publication Aug 08, 2023. Published online Sep 18, 2023.
doi: 10.21037/qims-23-101
View this article at: https://dx.doi.org/10.21037/qims-23-101

Introduction

Computed tomography angiography (CTA) is widely accepted as the first-line imaging modality for screening and diagnosing aortic aneurysm and acute aortic syndrome, including aortic dissection (AD), intramural hematoma (IMH), and penetrating atherosclerotic ulcer (1-3). Furthermore, due to its superiority in acquiring a timely and precise anatomical description, aortic CTA is also recommended for follow-up surveillance and postoperative complication assessment for cardiothoracic surgeries (4,5).

Typically, any patient with AD should to undergo follow-up CTA 3 or 4 times in the first year after the operation (6). Such a large volume of contrast medium, necessitated by the baseline and frequent follow-up CTA, inevitably poses an increased risk of contrast-induced nephropathy, particularly for patients with renal insufficiency (7,8). Unfortunately, steeply reducing the dose of contrast medium affects image quality and hinders a diagnosis from being made. Therefore, the means to obtaining ideal image quality with ultra-low dose contrast remains an area of essential research.

Technically, vessel enhancement relies on the concentration of iodine contrast medium, which is artificially injected to increase the difference in its X-ray absorption from the surrounding soft tissue. Dual-energy CT (DECT) can potentially increase vessel enhancement via virtual monochromatic image (VMI) reconstruction at a lower energy level, thus improving vessel contrast against the soft tissue. Previous CTA studies attempted this process and achieved a 30–50% reduction in contrast without significantly impacting image quality. Nevertheless, image quality was sacrificed to only a diagnosable level when the contrast was reduced by more than 70%. Therefore, a more stable method of simultaneously conserving contrast and retaining image quality is needed (9-12). Moreover, the traditional source-based DECT only is adapted to fixed tube voltage for dual-energy imaging (13). Its lack of flexibility in the protocol also interrupts the habitual workflow of CTA examinations.

Detector-based dual-layer spectral CT (DLCT) offers a new method for acquiring energy CT images via retrospective reconstruction with a single scan (14). The single X-ray detector system allows for high spatial and temporal resolution for VMI (15). A half-reduced contrast dose in coronary artery CTA with the VMI derived from DLCT has demonstrated good image quality (16). However, its usage in aortic CTA is rare. We hypothesized that a more significant reduction in the contrast (i.e., over 70%) without a significant impairment to image quality could be realized using DLCT. Considering that previous studies and some phantom studies have indicated 40-keV [which is close to the iodine K-edge (33-keV)] as an ideal energy level used for spectral CT (11,17,18), we aimed to investigate the feasibility of an ultra-low iodine dose protocol for aortic CTA examinations on DLCT. In addition, virtual noncontrast (VNC) images derived from DECT allow for the possibility of saving a noncontrast CT scan in routine clinical use. Thus, we aimed to clarify the relationship between VNC in different contrast protocols by referring to the true noncontrast (TNC) images.

Methods

Study population

This study was conducted in accordance with the Declaration of Helsinki (as revised in 2013), approved by the Ethics Committee of West China Hospital of Sichuan University, and registered at National Institute of Clinical Research (No. ChiCTR1900028475). Written informed consent was obtained from all patients.

We prospectively recruited 37 adult patients referred for aortic CTA examination at a single center from May 2022 to August 2022. Patients who were eligible for aortic CTA examination were included. The exclusion criteria were (I) inability to finish breath-holding during the examination (such as with severe pulmonary disease, heart failure, unconsciousness, or restlessness), (II) allergy to contrast medium or evidence of renal insufficiency (estimated glomerular filtration rate <60 mL/minute/1.73 m^2 or serum creatinine level ≥120 mmol/L), (III) pregnancy, and (IV) refusal to participate. Data on demographics (age, sex), height, weight, and the reasons for aortic CTA were collected once the patient was enrolled in the study.

Image acquisition and reconstruction

DLCT scans were performed using a dual-layer detector spectral CT (CT 7500, Philips Healthcare, Amsterdam, The Netherlands). All patients underwent noncontrast, low- and full-dose contrast scans from the superior thoracic inlet to the pubic symphysis. All scans were conducted under the following parameters: low tube voltage (100 kVp), automatic tube current adapted to the patient size (DoseRight, Philips Healthcare; reference tube current 50–300 mAs), collimation 128×0.625 mm, and rotation time 0.27 seconds.

After a noncontrast scan, the bolus-tracking technique was used with a delay of 4 s when the trigger threshold reached 100 Hounsfield units (HU) in the descending aorta (DAO) at the level of the pulmonary artery. For the low-dose contrast CTA, a standard volume mixture (25% nonionic contrast medium of 400 mgI/mL of iomeprol; 75% saline administered via high-pressure syringe) was injected at a 4.5 mL/s flow rate, which was followed by injection of 30 mL of saline at the same flow rate. The full-dose CTA was then performed using a normal volume (1 mL/kg) of the same contrast medium at the same flow rate, which was followed by an injection of 30 mL of saline (with an approximately 2- to 3-minute delay) after the low-dose CTA.

After all the examinations, the spectral base image (SBI) data were automatically reconstructed and reviewed using the workstation (IntelliSpace Portal 10.0, Philips Healthcare). Multiparameter spectral low-dose images were retrospectively generated from the SBI. Based on previous studies, 40-keV was considered to be the most optimal level for the greater enhancement of vessels, and 70-keV was the closest level to conventional images. Thus, VMI at 40- and 70-keV was chosen and compared against the full-dose images (19-22). VNC images were then reconstructed for the low-dose (VNC_{low}) and full-dose (VNC_{full}) groups and compared to the conventional CT noncontrast images. The complete study protocol is presented in *Figure 1*.

Post-processing and imaging analysis

The image quality of the aorta and branches was independently assessed based on axial-view reconstructed images by two experienced radiologists with over 10 years of experience in aortic CTA diagnosis. The radiologists independently evaluated all images using a qualitative scoring system ranging from 1 to 5 points and assessed the 3D post-processing reconstruction images in terms of volume rendering, maximum intensity projection, and multiplanar reconstruction.

For objective analysis of the vessel attenuation, 3 circular regions of interest (ROIs) with the same diameter (100 mm^2) were drawn at the aortic root level for the ascending aorta (AAO), at the pulmonary artery bifurcation level for the DAO, and at the abdominal trunk level for the abdominal aorta (AA) to acquire the mean CT value (CT_{vessel}) as vessel attenuation and the corresponding standard deviation (SD_{vessel}). The vessels' signal-to-noise ratio (SNR) was calculated as follows: $SNR = CT_{vessel}/SD_{vessel}$. Subsequently, background ROIs were placed at the paravertebral muscles at the corresponding AAO, DAO, and AA levels to acquire the attenuation of the muscles (CT_{muscle}) and image noise (SD_{muscle}). Contrast-to-noise ratio (CNR) was defined as follows: $CNR = (CT_{vessel} - CT_{muscle})/SD_{muscle}$.

Once the above measurements for one group were completed, the ROIs would be copied to measure the parameters for the other two groups of images. Notably, that true lumen was selected to place the ROIs, and all levels were carefully chosen to avoid any impact from metallic or motion artifacts or calcified plaques.

To quantitatively measure the VNC image quality, we used the differences between vessel attenuation and the

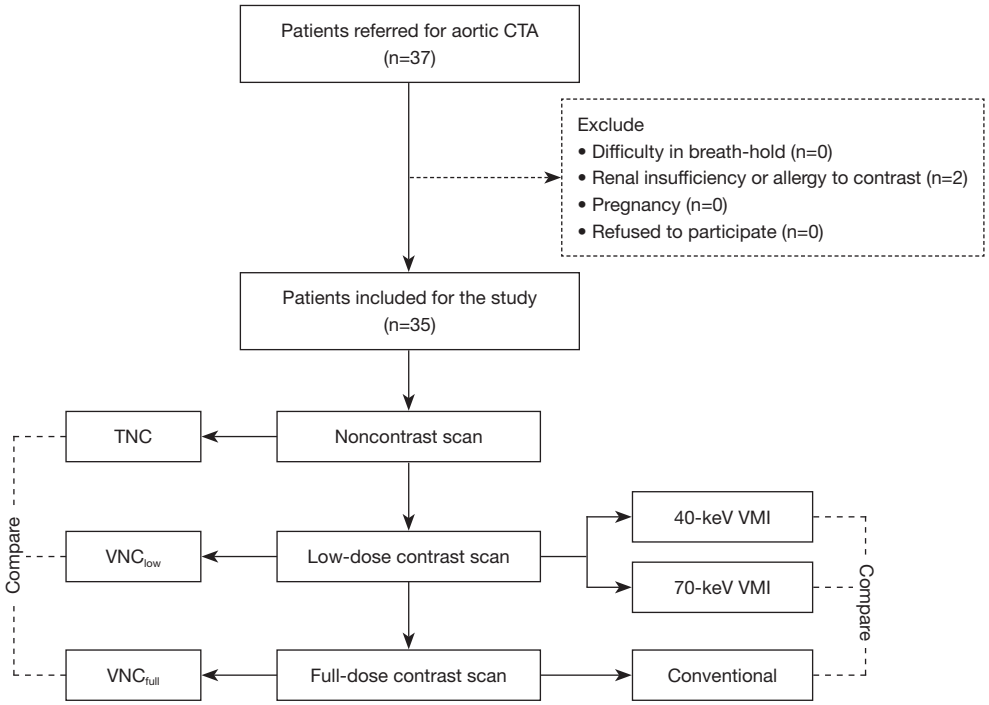

Figure 1 Flowchart of the study. CTA, computed tomography angiography; TNC, true noncontrast; VNC, virtual noncontrast; VMI, virtual monochromatic image.

muscle to determine the efficacy of VNC iodine removal as compared with that of the TNC. The defined parameters were (I) vessel-muscle contrast (VMC), calculated as ($CT_{vessel} - CT_{muscle}$); (II) vessel:muscle ratio (VMR), calculated as CT_{vessel}/CT_{muscle}; and (III) vessel-muscle percentage (VMP), calculated as $(CT_{vessel} - CT_{muscle})/CT_{muscle} \times 100\%$.

A 5-point grading system was used for subjective quality analysis to grade vessel enhancement and image noise quality. For vessel enhancement, (I) a score of 1 denoted poor vessel opacification and inadequate delineation between the vessel and its surrounding tissue, (II) a score of 2 denoted suboptimal vessel opacification and blurring of the vessel margin, (III) a score of 3 denoted acceptable vessel opacification for diagnosis and moderate blurring of the vessel margin, (IV) a score of 4 denoted good vessel opacification and slight blurring of the vessel margin, and (V) a score of 5 denoted excellent vessel opacification and a clear vessel margin. Similarly, image noise was also graded by a 5-point grading system: (I) a score of 1 denoted severe image noise; (II) a score of 2 denoted substantial image noise; (III) a score of 3 denoted moderate image noise; (IV) a score of 4 denoted mild image noise; and (V) a score of 5 denoted very low or negligible image noise (23).

Endpoints

The CNR and SNR of the 40-keV VMI derived from the ultra-low iodine dose protocol that we developed for aortic CTA examinations was used as the primary endpoint of this study.

Subjective image quality, including scores for enhancement and noise of the 40-keV VMI, was used as the secondary endpoint. Furthermore, the indices used to evaluate the image quality of the VNC image (VMC, VMR, and VMP) were used as exploratory endpoints.

Statistical analysis

Continuous data are expressed as the mean ± standard deviation (SD). Normal distribution was tested using the Shapiro-Wilk test. The significance of differences between the three groups was calculated using analysis of variance (ANOVA). The 1-way ANOVA test was used to compare the objective image quality analysis data, and post hoc analysis with Bonferroni correction was applied to adjust for the multiple comparisons. Categorical data are expressed as frequencies and the corresponding percentages. Bland-

Table 1 Demographic data of the patients

Variables	Value
Age (years)	54±11
Sex (male/female)	28/7
Height (cm)	165.3±9.1
Weight (kg)	68.2±10.76
BMI (kg/m^2)	24.9±2.8
Reason for examination	
Post-surgery of type A AD	15
Post-surgery of type B AD	9
Aortic aneurysm	7
Aortic aneurysmal dilation	1
Acute intramural hematoma	2
Post-surgery of TAVI	1

Data are presented as the mean ± standard deviation or number. BMI, body mass index; AD, aortic dissection; TAVI, transcatheter aortic valve implantation.

Altman analysis and interclass correlation coefficient (ICC) were applied to evaluate the reproducibility of CT value measurement. A P value less than 0.05 was considered statistically significant. All statistical analyses were performed with the R software (v. 3.3.1, The R Foundation for Statistical Computing; https://www.R-project.org/).

Results

Patient characteristics

After 2 patients were excluded due to renal insufficiency, 35 patients (28 males, 7 females; mean age 54 years) were ultimately included in this study. The mean body mass index (BMI) was 24.9 kg/m^2. There were 30 cases of postoperative AD (including 15 type A AD cases, 9 type B AD cases, 4 aneurysm cases, and 2 IMH cases), 1 case of transaortic valve implantation (TAVI), and 4 cases of acute aortic syndrome (including 3 aortic aneurysm cases and 1 aortic aneurysmal dilation case) (*Table 1*).

Objective and subjective image quality analysis

None of the CNRs of the 40-keV VMI were lower than those of full-dose images, and they were significantly higher than those of the 70-keV VMI. Furthermore, the SNR of the 40-keV images exceeded those of the full-dose images at the AAO (40-keV VMI *vs.* full-dose images: 32.7±7.4 *vs.* 24.5±6.1; P<0.05) and DAO (40-keV VMI *vs.* full-dose images: 28.2±8.3 *vs.* 20.8±5.8; P<0.05). Moreover, they achieved only a numerical difference at the AA (40-keV VMI *vs.* full-dose images: 21.1±6.2 *vs.* 18.2±5.9; P>0.05).

In addition, the CT value was slightly lower in the 40-keV VMI than in the full-dose images but significantly higher than in the 70-keV images. Regarding noise, VMI for both 40- and 70-keV had less noise than did the full-dose images, but the 40-keV VMI showed a slightly higher noise level at the AAO and DAO than did the 70-keV VMI (*Table 2* and *Figure 2*).

For vessel enhancement, although the conventional images looks naturally better, there were no significant differences between the 40-keV and full-dose images observed at any of the aortic sites (aorta: 4.37±0.46 *vs.* 4.57±0.48, P=0.096; brachiocephalic artery: 4.34±0.45 *vs.* 4.51±0.49, P=0.152; abdominal aortic side branch: 4.42±0.48 *vs.* 4.51±0.49, P=0.480). However, the above two groups of images had significantly higher vessel enhancement scores than did the 70-keV group. Notably, the image noise score of the 40-keV VMI was statistically higher than that of both the full-dose images and VMI (all P values <0.001) (*Table 3*).

Comparison between VNC and TNC images

As presented in *Table 4*, the VNC_{low} images were closer to the TNC images in VMC, VMR, and VMP and statistically different from the VNC_{full} images (P<0.001). No statistical difference was observed between the VNC_{low} and TNC images at the DAO level. At the AAO level, the VNC_{low} images were similar to TNC in terms of VMR and VMP. However, at the AA level, the VNC_{low} images were still significantly different from the TNC images. Subjectively, qualitative analysis of the images also demonstrated that the VNC_{low} images were more similar to the TNC images than were the VNC_{full} images (*Figure 3*).

Reproducibility of the CT value measurements

Measurements of the CT value demonstrated moderate-to-good interobserver agreement (ICC range, 0.712–0.932) with narrow limits of agreement in the Bland-Altman analyses (Figure S1).

Table 2 Comparison of objective image quality items among the 40- and 70-keV low-dose contrast VMI and full-dose contrast images

Item	40-keV VMI	70-keV VMI	Full-dose image	P value
Attenuation (HU)				
AAO	452.3±72.5*†	152.8±22.1*	502.8±81.5	<0.001
DAO	434.1±61.6*†	151.3±17.9*	435.9±65.8	<0.001
AA	410.5±63.2*†	148.0±19.4*	453.9±67.1	<0.001
Noise (HU)				
AAO	14.1±2.7*†	12.0±1.4*	21.2±4.8	<0.001
DAO	16.1±3.3*†	13.8±2.2*	22.7±4.2	<0.001
AA	20.2±3.5*	18.4±3.3*	26.4±5.5	<0.001
SNR				
AAO	32.7±7.4*†	12.8±2.6*	24.5±6.1	<0.001
DAO	28.2±8.3*†	11.2±2.6*	20.8±5.8	<0.001
AA	21.1±6.2†	8.2±2.2*	18.2±5.9	<0.001
CNR				
AAO	20.7±7.6†	6.9±2.3*	19.0±5.5	<0.001
DAO	21.4±7.4†	7.3±2.8*	19.7±7.8	<0.001
AA	21.4±6.5†	6.1±2.4*	21.2±6.1	<0.001

Data are presented as the mean ± standard deviation. *, significant difference from the full-dose group; †, significant difference from the 70-keV VMI group. VMI, virtual monochromatic image; HU, Hounsfield units; AAO, ascending aorta; DAO, descending aorta; AA, abdominal aorta; SNR, signal-to-noise ratio; CNR, contrast-to-noise ratio.

Radiation and contrast dose

The mean radiation dose used for each scan included a dose length product (DLP) of 449.4±66.6 mGy·cm and an effective dose (ED) of 6.74±1.0 mSv. A mean 85.85± 11.04 mL contrast dose was used for each case, including 17.05±2.19 mL used for the ultra-low contrast dose protocol and 68.08±8.88 mL for the full-dose protocol.

Discussion

This study demonstrated the excellent and comparable full-dose contrast image quality of the 40-keV VMI acquired from a 75%-contrast dose cutoff aortic CTA protocol on spectral CT. Furthermore, we found that the VNC images reconstructed from the ultra-low dose protocol were much closer to those of the TNC images than were those of the VNC images from the full-dose protocol. The ultra-low dose protocol for aortic CTA might be an option for patients who have or at risk of renal insufficiency.

The 40-keV VMI reconstructed from the ultra-low-dose contrast CTA scan showed noninferior image quality to the ones acquired through the full-dose contrast CTA scan. Our developed protocol achieved both ideal image quality and the lowest contrast dose compared to previous studies (11). In addition, since the full- and low-dose VMI was acquired from the same individual, our study yielded additional evidence regarding the optimal vessel enhancement and low image noise of the 40-keV VMI compared to the ultra-low-dose contrast protocol. The retained enhancement of the 40-keV VMI with ultra-low dose contrast was primarily attributed to the energy level at 40-keV being closer to the K-edge of iodine. Thus, the contrast between the vessel and background tissue was amplified, as demonstrated by the significant improvement in vessel enhancement from 70- to 40-keV VMI. Similar results were seen in coronary CTA and lower extremity runoff studies using dual-energy CT (24). Wichmann *et al*. used polychromatic CT aortography to achieve a 70% cutoff but reported barely satisfactory subjective image quality (25). Traditionally, lowering the tube voltage can achieve a contrast dose reduction.

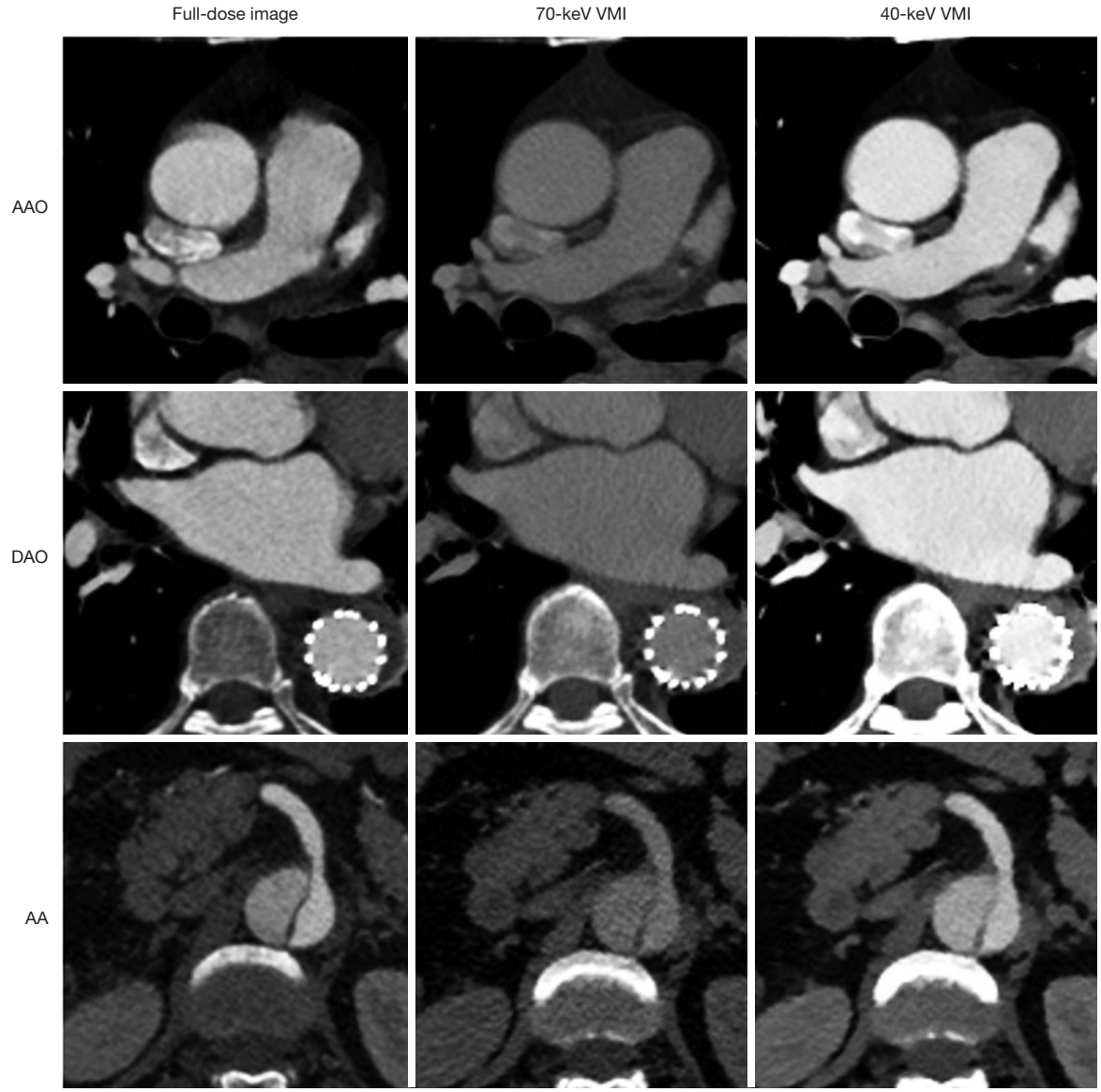

Figure 2 Case-based comparison of the CT angiography images among the full-dose image, 70-keV VMI, and 40-keV VMI groups at the AAO, DAO, and AA levels. Note that the vessel enhancement of the 40-keV images was similar to that of the conventional images, and the enhancement of the above 2 was significantly better than that of the 70-keV images. White dotted circles indicate an implanted stent. VMI, virtual monochromatic image; AAO, ascending aorta; DAO, descending aorta; AA, abdominal aorta; CT, computed tomography.

However, this cannot achieve a greatly reduced amount of contrast, as it is limited by the basic requirements for X-ray penetration. Frequent follow-up CTA scans are necessary for patients with aortic diseases. Using the ultra-low contrast scan, we achieved an average reduction of 51 mL (nearly 80%) of contrast. Thus, the crucial contribution of this study is the novel development of a potential ultra-low contrast protocol for the aortic CTA scan, which was validated through a rigorous self-contrast study design.

Another interesting finding of our study is that the VNC images derived from our ultra-low protocol were similar to the TNC images but had superior image quality and much less contrast medium remanence than those from the full-dose contrast protocol. This finding suggests that a VNC image derived from an ultra-low iodine protocol could

Table 3 Comparison of subjective image quality items among the 40- and 70-keV low-dose contrast VMI and full-dose contrast images

Item	1	2	3	4	5	Mean score
Aortic enhancement, n (%)						
40-keV VMI	0 (0.0)	0 (0.0)	0 (0.0)	22 (62.9)	13 (37.1)	4.37
70-keV VMI	7 (20.0)	10 (28.6)	18 (51.4)	0 (0.0)	0 (0.0)	2.31
Full-dose image	0 (0.0)	0 (0.0)	0 (0.0)	15 (42.9)	20 (57.1)	4.57
Brachiocephalic enhancement, n (%)						
40-keV VMI	0 (0.0)	0 (0.0)	0 (0.0)	23 (65.7)	12 (34.3)	4.34
70-keV VMI	0 (0.0)	23 (65.7)	12 (34.3)	0 (0.0)	0 (0.0)	2.34
Full-dose image	0 (0.0)	0 (0.0)	0 (0.0)	17 (48.6)	18 (51.4)	4.51
Abdominal aortic side branch enhancement, n (%)						
40-keV VMI	0 (0.0)	0 (0.0)	0 (0.0)	20 (57.1)	15 (42.9)	4.42
70-keV VMI	8 (22.8)	11 (31.4)	16 (45.8)	0 (0.0)	0 (0.0)	2.22
Full-dose image	0 (0.0)	0 (0.0)	0 (0.0)	17 (48.6)	18 (51.4)	4.51
Overall image noise, n (%)						
40-keV VMI	0 (0.0)	0 (0.0)	0 (0.0)	10 (28.5)	25 (71.5)	4.71
70-keV VMI	0 (0.0)	0 (0.0)	0 (0.0)	29 (82.8)	6 (17.2)	4.17
Full-dose image	0 (0.0)	0 (0.0)	0 (0.0)	25 (71.5)	10 (28.5)	4.28

Numbers 1–5 represent the scores of each subjective evaluation index. VMI, virtual monochromatic image.

Table 4 Comparison of VNC images derived from low-dose and full-dose contrast images

Item	VNC_{low}	VNC_{full}	TNC	P value
VMC				
AAO	3.48±9.16*†	21.10±12.94*	−4.40±16.28	<0.001
DAO	−0.04±9.27	22.58±12.96*	−4.73±11.92	<0.001
AA	1.45±7.00*†	25.57±11.63*	−6.15±9.01	<0.001
VMR				
AAO	1.17±0.33	1.92±0.81*	1.00±0.41	<0.001
DAO	1.02±0.26	1.79±0.61*	0.93±0.21	<0.001
AA	1.04±0.17*†	1.65±0.32*	0.89±0.16	<0.001
VMP				
AAO	0.17±0.33	0.92±0.81*	0.01±0.41	<0.001
DAO	0.02±0.61	0.79±0.61*	−0.06±0.21	<0.001
AA	0.44±0.17*†	0.62±0.32*	−0.01±0.16	<0.001

Data are presented as the mean ± standard deviation. *, significant difference from the TNC group; †, significant difference from the VNC_{full} group. TNC, true noncontrast; VNC, virtual noncontrast; VMC, vessel-muscle contrast; AAO, ascending aorta; DAO, descending aorta; AA, abdominal aorta; VMR, vessel:muscle ratio; VMP, vessel-muscle percentage.

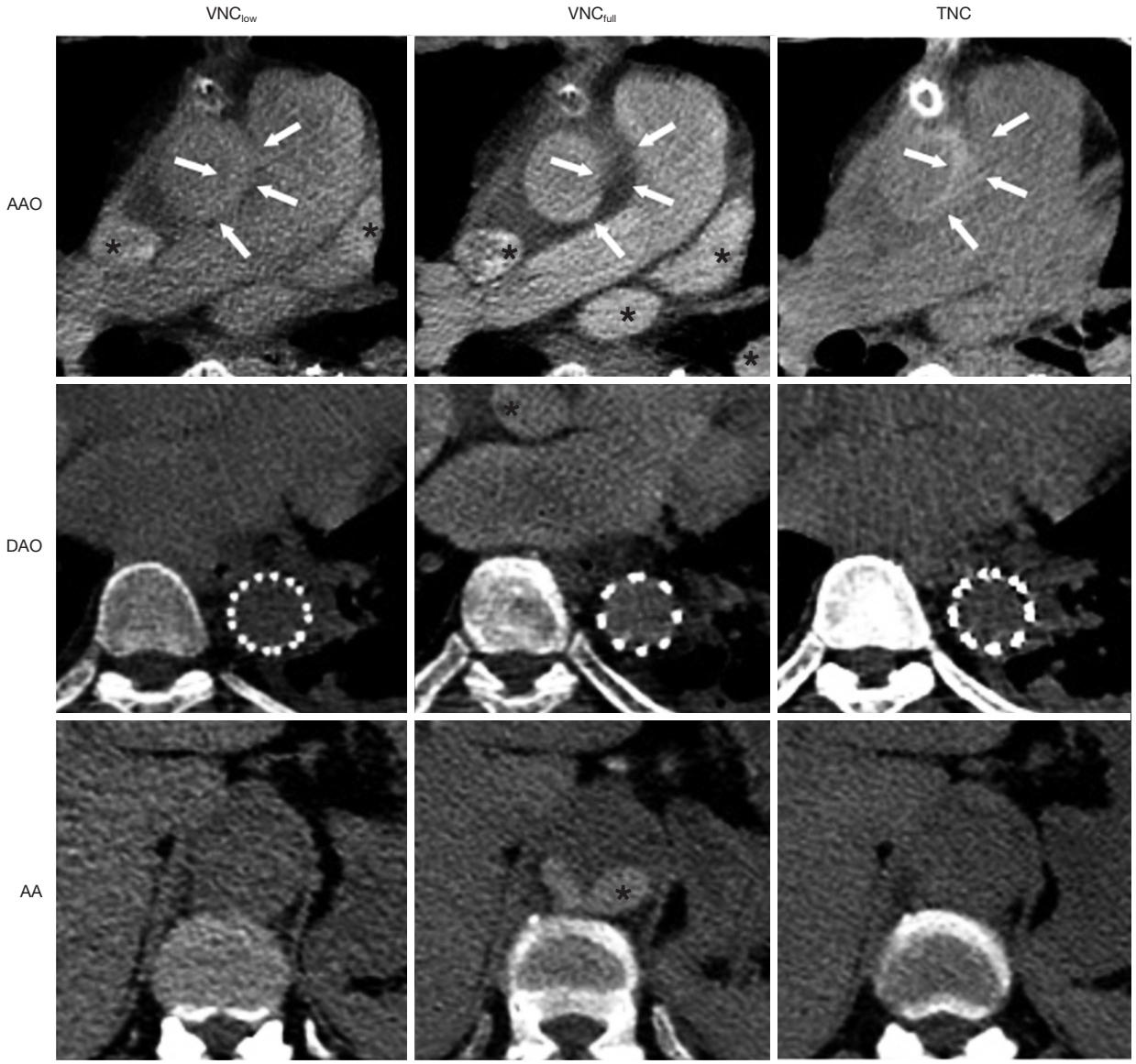

Figure 3 Case-based comparison of the VNC images derived from the 75% cutoff ultra-low (VNC$_{low}$) and standard full dose (VNC$_{full}$) contrast protocol with reference to the TNC images at the AAO, DAO, and AA levels. Note that significant remnants of iodine (black asterisk) could be found in the VNC$_{full}$ images, but only slight amounts were found in the VNC$_{low}$ images. In addition, the intramural hematoma (arrows) of clinical significance could be found in the TNC and VNC$_{low}$ images but would be mistaken as a thrombus in the VNC$_{full}$ images. White dotted circles indicate an implanted stent. VNC, virtual noncontrast; TNC, true noncontrast; AAO, ascending aorta, DAO, descending aorta, AA, abdominal aorta.

replace the TNC image, thus avoiding the radiation from a noncontrast scan. Similar VNC results to those of our full-dose group can be found in the study by Lehti *et al.* who found that the VNC images reconstructed from a conventional full-dose protocol had a significantly higher mean attenuation and a higher noise level than did TNC and could not replace TNC in the confirmed diagnosis (26). Our results further indicate that a lower dose of CTA might produce better VNC and increase the probability of using VNC as a substitute. However, Sauter *et al.* proposed that

the concentration of contrast medium in blood vessels does not affect the reconstructive VNC quality (27). Nevertheless, their study only compared the VNC from the arterial and venous phase images. Theoretically, the VNC was reconstructed by deionizing iodine-containing tissues, and a previous study conducted by Van Hedent *et al.* also concluded that factors such as the patient's body size, radiation dose, and contrast dose can affect the quality of the VNC (28). Based on the results from this study, we believe that a lower contrast dose should produce better VNC images, but further investigations are warranted. In addition, whether the VNC derived from the ultra-low contrast protocol can replace TNC from a diagnostic viewpoint needs to be determined by further study.

Another attribute of the optimal VMI image quality at 40-keV might be the acceptable noise increase when the energy level is adjusted from 70- to 40-keV. The VMI image noise was inversely associated with the energy level. However, in DLCT, the noise of the 40-keV VMI was slightly worse than that of the 70-keV VMI at the AAO and DAO. This could be due to the innate mechanism of the spectral CT, in which exactly-matched dual-layer detectors are used to eliminate the correlated noise (15). Therefore, the SNR and CNR of the 40-keV VMI images were comparable to those of the full-dose images, even when the CT value was slightly lower than that of the full-dose images.

However, DLCT cannot achieve a radiation dose or a purer spectral separation as that of DECT based on the dual-source technique (29,30). In addition, limited by the 8-mm width, its use in fast or one-beat cardiac scanning is not applicable. Nevertheless, the above drawbacks do not significantly impact the aortic CTA, as shown in our study. Given the feasibility of spectral CT in the retrospective reconstruction of multiparameter images and their capacity to salvage poor-quality CTA, the clinical application of such an ultra-low contrast CTA protocol is promising, and further diagnostic validation studies are warranted.

This study had several limitations. First, despite the demonstrated image quality, a higher radiation dose associated with DECT compared to some low-dose protocols remains a concern. Second, aortic CTA has been accepted as the gold standard for anatomical assessment; thus, we used a self-control study to compare the image quality rigorously. Moreover, the scope of this investigation was limited to the assessment of vessel enhancement and image noise. Although good image quality was the basis for diagnosis, the results of this study should not yet be expanded to include diagnostic accuracy. Third, as a single-center design was employed, all individuals included were routine patients referred to aortic CTA. Although the comparison was rigorously designed, the cohort scale was limited. Finally, based on previous studies, we only selected the 40-keV level for a clinically efficient workflow, leaving the other energy levels unexamined.

With our developed ultra-low contrast dose aortic CTA scan protocol on DLCT, the 40-keV virtual monoenergy reconstructed images achieved comparable image quality to that of full-dose CTA. Furthermore, the VNC images from the ultra-low contrast dose protocol were closer to TNC images than were those from the full-dose protocol.

Conclusions

We developed an ultra-low contrast aortic CTA scan protocol on DLCT, in which the 40-keV virtual monenergy reconstructed images and the derived VNC images could achieve comparable image quality to that of full-dose CTA and noncontrast images.

Acknowledgments

Funding: This work was supported by the National Natural Science Foundation of China (grant Nos. 82200553 and 81900311) and the 1.3.5 Project for Disciplines of Excellence-Clinical Research Incubation Project, West China Hospital Sichuan University (grant No. ZYGD18019).

Footnote

Conflicts of Interest: All authors have completed the ICMJE uniform disclosure form (available at https://qims.amegroups.com/article/view/10.21037/qims-23-101/coif). SD and HL, employees of Philips Healthcare, contributed to the description of technical principles and image post-processing without impacting the research results. The other authors have no conflicts of interest to declare.

Ethical Statement: The authors are accountable for all aspects of the work in ensuring that questions related to the accuracy or integrity of any part of the work are appropriately investigated and resolved. This study was conducted in accordance with the Declaration of Helsinki (as

revised in 2013) and was approved by the Ethics Committee of West China Hospital of Sichuan University. Written informed consent was obtained from all patients.

References

1. Raff GL, Chinnaiyan KM, Cury RC, Garcia MT, Hecht HS, Hollander JE, O'Neil B, Taylor AJ, Hoffmann U; Society of Cardiovascular Computed Tomography Guidelines Committee. SCCT guidelines on the use of coronary computed tomographic angiography for patients presenting with acute chest pain to the emergency department: a report of the Society of Cardiovascular Computed Tomography Guidelines Committee. J Cardiovasc Comput Tomogr 2014;8:254-71.
2. Yu Y, Gao Y, Wei J, Liao F, Xiao Q, Zhang J, Yin W, Lu B. A Three-Dimensional Deep Convolutional Neural Network for Automatic Segmentation and Diameter Measurement of Type B Aortic Dissection. Korean J Radiol 2021;22:168-78.
3. Kim YJ, Yong HS, Kim SM, Kim JA, Yang DH, Hong YJ; Korean Society of Radiology; Korean Society of Cardiology. Korean guidelines for the appropriate use of cardiac CT. Korean J Radiol 2015;16:251-85.
4. Maisch B. The AHA/ACC/ASE/CHEST/SAEM/SCCT/SCMR guidelines 2021 on thoracic pain. Herz 2022;47:48-54.
5. MacGillivray TE, Gleason TG, Patel HJ, Aldea GS, Bavaria JE, Beaver TM, Chen EP, Czerny M, Estrera AL, Firestone S, Fischbein MP, Hughes GC, Hui DS, Kissoon K, Lawton JS, Pacini D, Reece TB, Roselli EE, Stulak J. The Society of Thoracic Surgeons/American Association for Thoracic Surgery Clinical Practice Guidelines on the Management of Type B Aortic Dissection. Ann Thorac Surg 2022;113:1073-92.
6. An KR, de Mestral C, Tam DY, Qiu F, Ouzounian M, Lindsay TF, Wijeysundera HC, Chung JC. Surveillance Imaging Following Acute Type A Aortic Dissection. J Am Coll Cardiol 2021;78:1863-71.
7. Faucon AL, Bobrie G, Clément O. Nephrotoxicity of iodinated contrast media: From pathophysiology to prevention strategies. Eur J Radiol 2019;116:231-41.
8. Canstein C, Korporaal JG. Reduction of contrast agent dose at low kV settings. White Paper. Siemens Healthcare GmbH, 2017.
9. Patino M, Parakh A, Lo GC, Agrawal M, Kambadakone AR, Oliveira GR, Sahani DV. Virtual Monochromatic Dual-Energy Aortoiliac CT Angiography With Reduced Iodine Dose: A Prospective Randomized Study. AJR Am J Roentgenol 2019;212:467-74.
10. Huang X, Gao S, Ma Y, Lu X, Jia Z, Hou Y. The optimal monoenergetic spectral image level of coronary computed tomography (CT) angiography on a dual-layer spectral detector CT with half-dose contrast media. Quant Imaging Med Surg 2020;10:592-603.
11. Cavallo AU, Patterson AJ, Thomas R, Alaiti MA, Attizzani GF, Laukamp K, Große Hokamp N, Bezerra H, Gilkeson R, Rajagopalan S. Low dose contrast CT for transcatheter aortic valve replacement assessment: Results from the prospective SPECTACULAR study (spectral CT assessment prior to TAVR). J Cardiovasc Comput Tomogr 2020;14:68-74.
12. Shuman WP, O'Malley RB, Busey JM, Ramos MM, Koprowicz KM. Prospective comparison of dual-energy CT aortography using 70% reduced iodine dose versus single-energy CT aortography using standard iodine dose in the same patient. Abdom Radiol (NY) 2017;42:759-65.
13. So A, Nicolaou S. Spectral Computed Tomography: Fundamental Principles and Recent Developments. Korean J Radiol 2021;22:86-96.
14. Zopfs D, Rinneburger M, Pinto Dos Santos D, Reimer RP, Laukamp KR, Maintz D, Lennartz S, Große Hokamp N. Evaluating anemia using contrast-enhanced spectral detector CT of the chest in a large cohort of 522 patients. Eur Radiol 2021;31:4350-7.
15. Rajiah P, Rong R, Martinez-Rios C, Rassouli N, Landeras L. Benefit and clinical significance of retrospectively obtained spectral data with a novel detector-based spectral computed tomography - Initial experiences and results. Clin Imaging 2018;49:65-72.
16. Huang X, Gao S, Ma Y, Lu X, Jia Z, Hou Y. The optimal monoenergetic spectral image level of coronary computed tomography (CT) angiography on a dual-layer spectral detector CT with half-dose contrast media. Quant Imaging Med Surg 2020;10:592-603.
17. Sellerer T, Noël PB, Patino M, Parakh A, Ehn S, Zeiter

S, Holz JA, Hammel J, Fingerle AA, Pfeiffer F, Maintz D, Rummeny EJ, Muenzel D, Sahani DV. Dual-energy CT: a phantom comparison of different platforms for abdominal imaging. Eur Radiol 2018;28:2745-55.
18. Al-Baldawi Y, Große Hokamp N, Haneder S, Steinhauser S, Püsken M, Persigehl T, Maintz D, Wybranski C. Virtual mono-energetic images and iterative image reconstruction: abdominal vessel imaging in the era of spectral detector CT. Clin Radiol 2020;75:641.e9-641.e18.
19. Yin XP, Gao BL, Li CY, Zhou H, Zhao L, Zheng YT, Zhao YX. Optimal Monochromatic Imaging of Spectral Computed Tomography Potentially Improves the Quality of Hepatic Vascular Imaging. Korean J Radiol 2018;19:578-84.
20. Tanoue S, Nakaura T, Nagayama Y, Uetani H, Ikeda O, Yamashita Y. Virtual Monochromatic Image Quality from Dual-Layer Dual-Energy Computed Tomography for Detecting Brain Tumors. Korean J Radiol 2021;22:951-8.
21. Doerner J, Luetkens JA, Iuga AI, Byrtus J, Haneder S, Maintz D, Hickethier T. Poly-energetic and virtual mono-energetic images from a novel dual-layer spectral detector CT: optimization of window settings is crucial to improve subjective image quality in abdominal CT angiographies. Abdom Radiol (NY) 2018;43:742-50.
22. Nagayama Y, Tanoue S, Inoue T, Oda S, Nakaura T, Utsunomiya D, Yamashita Y. Dual-layer spectral CT improves image quality of multiphasic pancreas CT in patients with pancreatic ductal adenocarcinoma. Eur Radiol 2020;30:394-403.
23. Li W, You Y, Zhong S, Shuai T, Liao K, Yu J, Zhao J, Li Z, Lu C. Image quality assessment of artificial intelligence iterative reconstruction for low dose aortic CTA: A feasibility study of 70 kVp and reduced contrast medium volume. Eur J Radiol 2022;149:110221.
24. Yi Y, Zhao XM, Wu RZ, Wang Y, Vembar M, Jin ZY, Wang YN. Low Dose and Low Contrast Medium Coronary CT Angiography Using Dual-Layer Spectral Detector CT. Int Heart J 2019;60:608-17.
25. Wichmann JL, Gillott MR, De Cecco CN, Mangold S, Varga-Szemes A, Yamada R, Otani K, Canstein C, Fuller SR, Vogl TJ, Todoran TM, Schoepf UJ. Dual-Energy Computed Tomography Angiography of the Lower Extremity Runoff: Impact of Noise-Optimized Virtual Monochromatic Imaging on Image Quality and Diagnostic Accuracy. Invest Radiol 2016;51:139-46.
26. Lehti L, Söderberg M, Höglund P, Nyman U, Gottsäter A, Wassélius J. Reliability of virtual non-contrast computed tomography angiography: comparing it with the real deal. Acta Radiol Open 2018;7:2058460118790115.
27. Sauter AP, Muenzel D, Dangelmaier J, Braren R, Pfeiffer F, Rummeny EJ, Noël PB, Fingerle AA. Dual-layer spectral computed tomography: Virtual non-contrast in comparison to true non-contrast images. Eur J Radiol 2018;104:108-14.
28. Van Hedent S, Tatsuoka C, Carr S, Laukamp KR, Eck B, Große Hokamp N, Kessner R, Ros P, Jordan D. Impact of Patient Size and Radiation Dose on Accuracy and Precision of Iodine Quantification and Virtual Noncontrast Values in Dual-layer Detector CT-A Phantom Study. Acad Radiol 2020;27:409-20.
29. Albrecht MH, Vogl TJ, Martin SS, Nance JW, Duguay TM, Wichmann JL, De Cecco CN, Varga-Szemes A, van Assen M, Tesche C, Schoepf UJ. Review of Clinical Applications for Virtual Monoenergetic Dual-Energy CT. Radiology 2019;293:260-71.
30. Patino M, Prochowski A, Agrawal MD, Simeone FJ, Gupta R, Hahn PF, Sahani DV. Material Separation Using Dual-Energy CT: Current and Emerging Applications. Radiographics 2016;36:1087-105.

Cite this article as: Wang A, Li W, Huang W, Luo M, Xiao W, Qin C, Dong S, Liu H, Li Z, Diao K. Dual-layer spectral computed tomography aortography using a seventy-five-percent-reduced iodine dose protocol and multiparameter spectral imaging: comparison with conventional computed tomography imaging. Quant Imaging Med Surg 2023;13(10):6456-6467. doi: 10.21037/qims-23-101

